Supplementary Information (SI) for Soft Matter.
This journal is © The Royal Society of Chemistry 2026

Supporting Information to

Following the Formation of Single-Chain Nanoparticles Generated by Interblock Crosslinking within Diblock Copolymers: A Monte Carlo Simulation Study with Adjustable Interaction Strength between the Blocks

Anja Voigt, Christian Strauch, Tom Höfken, Mirco Wahab, Wiebke Hadwich, Christopher Barner-Kowollik, Conrad Hübler, Stefanie Schneider* and Felix A. Plamper*

Chain Folding

The collapse of a single chain is shown in Figure S1[1] and in Figure S2.

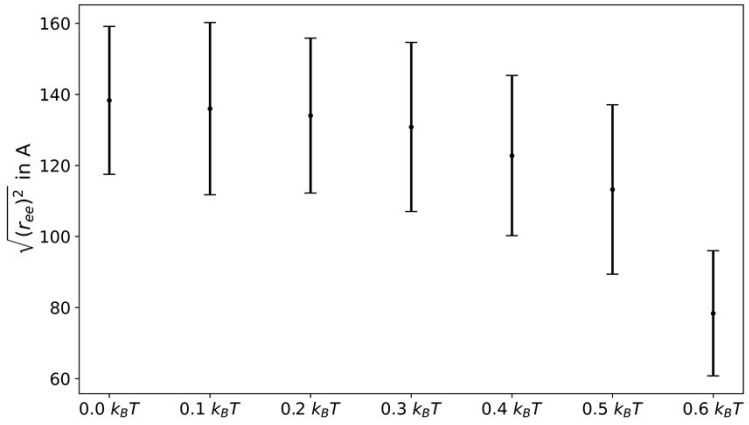

(a) End-to-end-distances

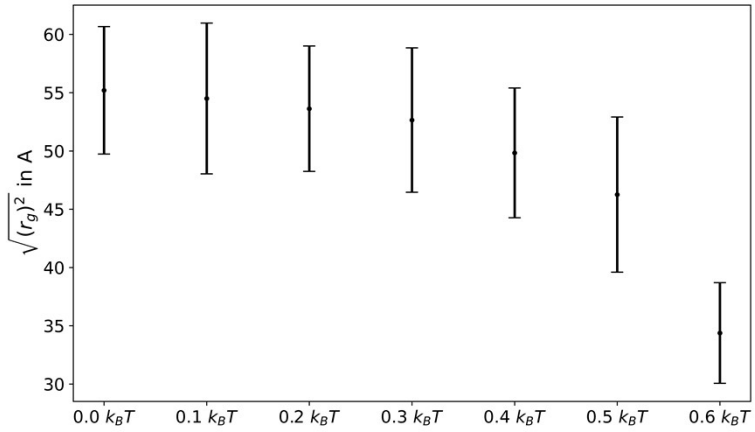

(b) Radii of gyration

Fig. S1: Change of end-to-end distances[1] and radii of gyration uponincreasing the interblock interaction energy between the beads of the two opposing blocks of a symmetric block copolymer (with hundred beads / block; the error bars indicate the standard deviation of the investigated structures).

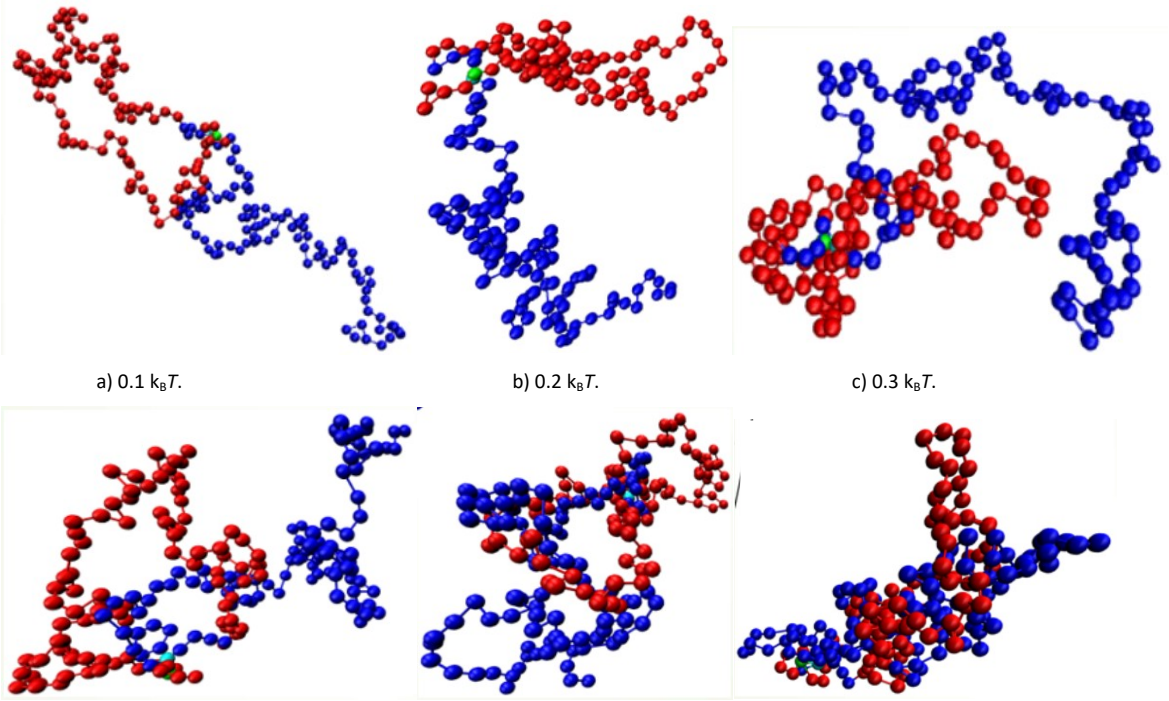

a) 0.1 k_BT. b) 0.2 k_BT. c) 0.3 k_BT.

d) 0.4 k_BT. e) 0.5 k_BT. f) 0.6 k_BT.

Fig. S2: Simulation snapshots showing the conformational changes upon increasing the potential depth ϵ of the interblock attractive potential between differently colored beads of a symmetric block copolymer (with hundred beads / block).

Contact Frequencies

We started with the analysis of the frequency of contacts between potentially crosslinkable monomer pairs for an interaction strength of $0.6\ k_BT$ (Fig. 2) in order to determine a suitable threshold radius (r_{distcl}) for the subsequent dynamic crosslinking simulations (which was then kept constant for most of the simulations). Later on, two crosslinkable beads are crosslinked if their distance is $\leq r_{distcl}$. These simulations were performed with suppressed crosslinking in our general simulation code (see "Model and simulation parameters" section for more details) to observe encounter frequencies without the formation of new bonds. The critical threshold radius was varied from 5.0 Å to 20.0 Å to assess the influence of spatial proximity required for potential crosslinking. The resulting heatmaps show that contacts between crosslinkable sites close to the block junction are generally more frequent because of their inherent proximity along the polymer chain (top left corner, Fig. S3). Furthermore, a pronounced tendency towards contacts in an antiparallel fashion along the block sequences (e.g. monomer 95 with 105, 85 with 115 and so on) is observed. This can be seen from a higher contact probability along a diagonal from the top left corner to the bottom right corner (compared to the upper right and lower left corner). This behaviour could be explained by a kind of zipping mechanism, where more likely contacts cooperatively facilitate the formation of further adjacent contacts.

Finally, a value of r_{distcl} = 6.0 Å was set for most of the subsequent simulations representing a balance between sufficient contact probability (~1%) and reasonable confinement for allowing sufficient equilibration before further crosslinking occurs inside the developing SCNPs. This reasoning is assisted by the histograms of the statistical contacts showing maxima at about 1 % for critical distances of 8 and 9 Å (see Fig. S4), as Fig. S4 indicates how often encounters with a certain contact frequency occur (there is always one outlier at highest contact frequencies, which relates to the contact between bead 95 and 105, but it is rather unlikely with 1 %, as it is just one contact option among 100 options).

Despite the maxima at approximately 1% at 8 and 9 Å (see Fig. S4), critical distances exceeding 6 Å $= 1.5 \cdot \sigma$ were not considered as realistic because the radius of the segments was 2 Å (bead diameter σ was 4 Å) so that an interaction over a distance of more than 3 segment radii could be easily disturbed by another particle moving through the bond or located near the bond. In addition, typical bond lengths to be set between two beads cannot be smaller than 4 Å as double segment radius. In the light of these findings, we chose a r_{distcl} = 6.0 Å as contact distance for the simulations with ϵ = 0.0 and $\epsilon = 0.6\ k_BT$ and r_{distcl} = 5.0 Å for the highest interaction energy of $\epsilon = 1.2\ k_BT$ in order to prevent full crosslinking already at the very beginning of the synthesis run.

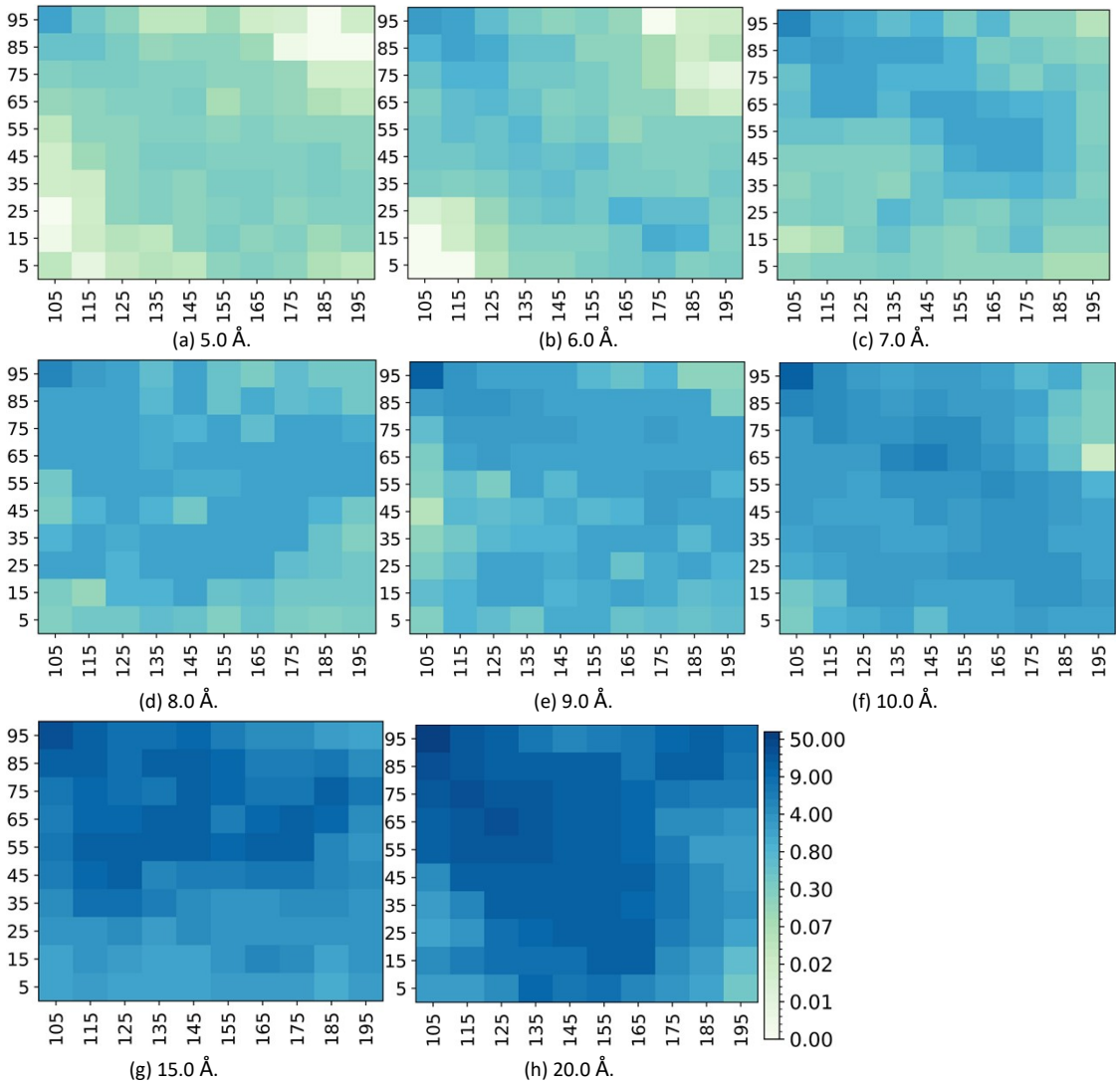

(a) 5.0 Å. (b) 6.0 Å. (c) 7.0 Å.

(d) 8.0 Å. (e) 9.0 Å. (f) 10.0 Å.

(g) 15.0 Å. (h) 20.0 Å.

Fig. S3: Heatmaps, where the "darkness" is proportional to the number of „interblock contacts" between crosslinkable beads; contact frequencies were analyzed for different contact threshold distances at $\epsilon = 0.6\ k_B T$; each square is assigned to one specific contact option.

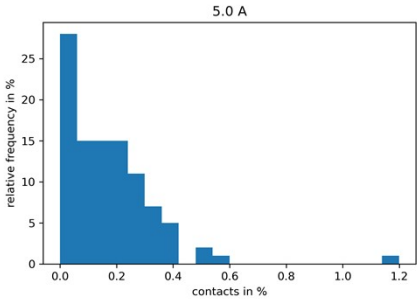

(a) 5.0 Å.

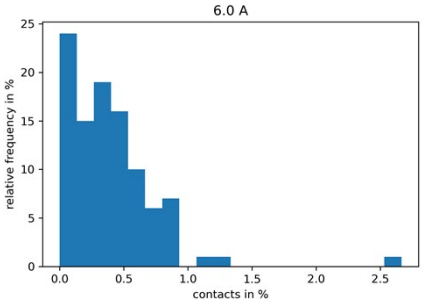

(b) 6.0 Å.

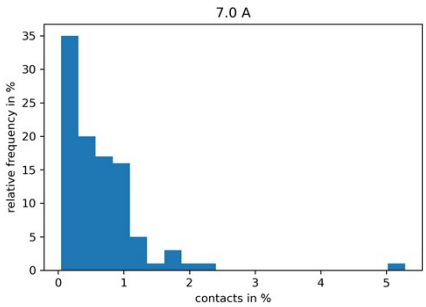

(c) 7.0 Å.

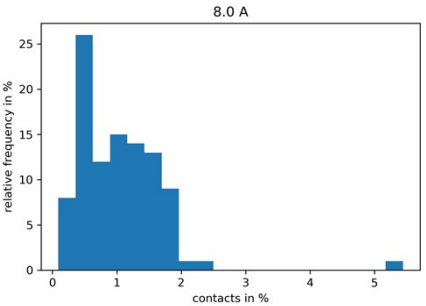

(d) 8.0 Å.

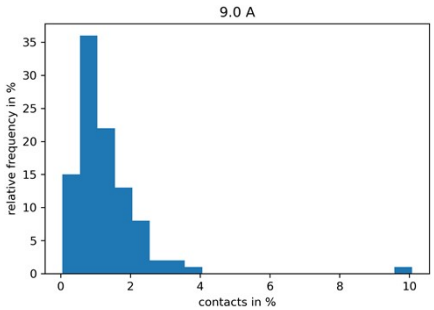

(e) 9.0 Å.

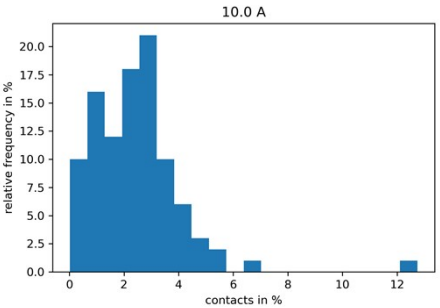

(f) 10.0 Å.

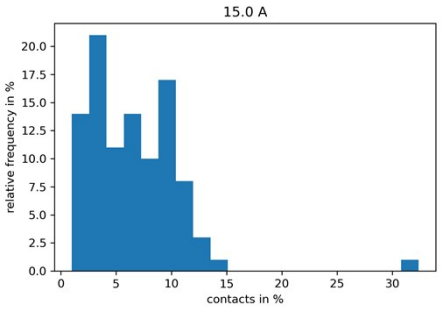

(g) 15.0 Å.

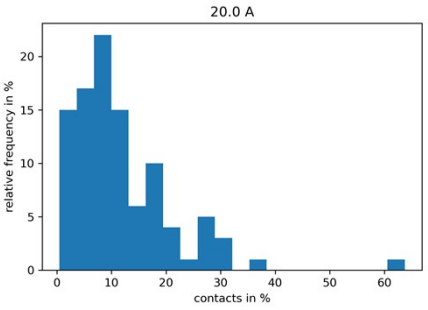

(h) 20.0 Å.

Fig. S4: Histograms of contact frequencies for critical distances.

Heat Maps

A more detailed view on Fig. 2 (g) in the main part is given in Fig. S5.

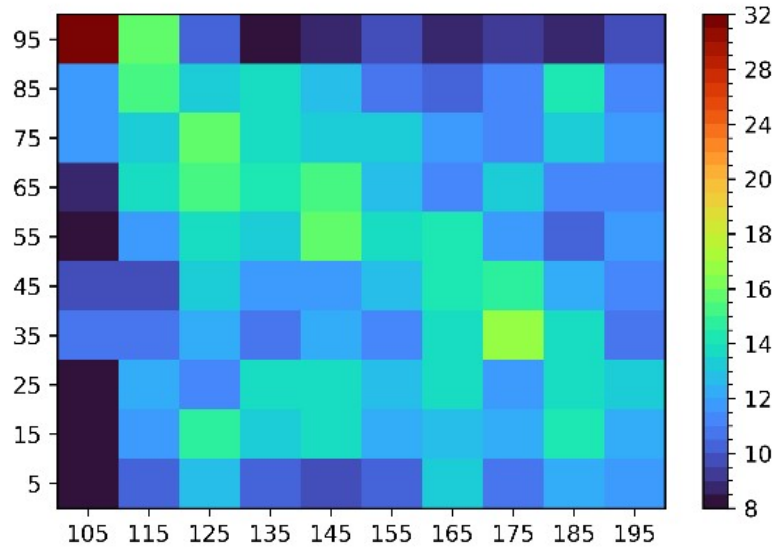

Fig. S5: Different color coding of Fig. 2 (g) in main part.

Compaction

A more detailed box plot than the one given in Fig. 5 (main part) is given in Fig. S7. The averages from the more detailed box plot are given in Fig. S6.

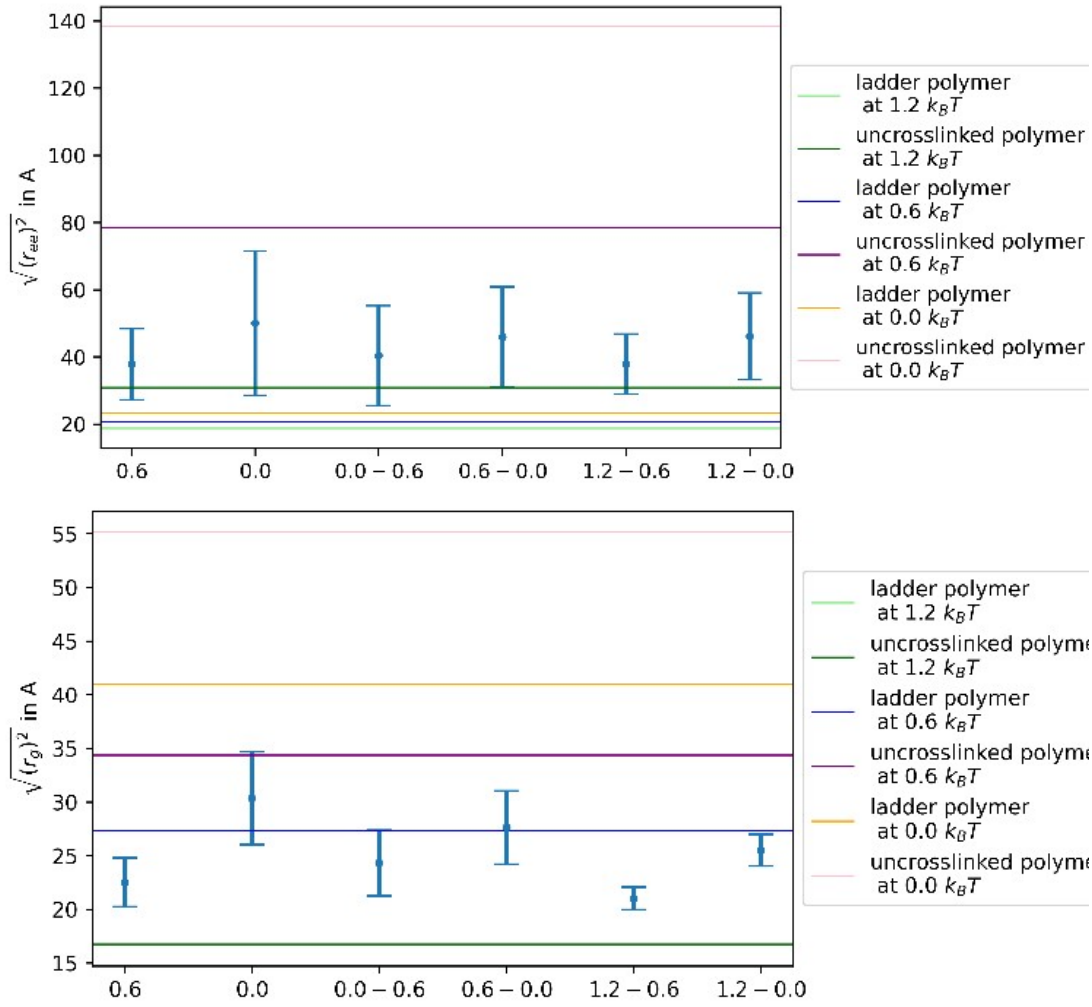

Fig. S6: Different representation of part of Fig. 5 (main part) with averages and standard deviation calculated from 200 different simulations (the indicated ϵ (in k_BT) in was kept both for dynamic SCNP synthesis and analysis after SCNP formation on the left hand side, while the synthesis conditions were reversed for the right hand side, i.e. "$0.0 - 0.6$" indicates a synthesis at $\epsilon = 0.0\ k_BT$, but an equilibration and analysis at $0.6\ k_BT$).

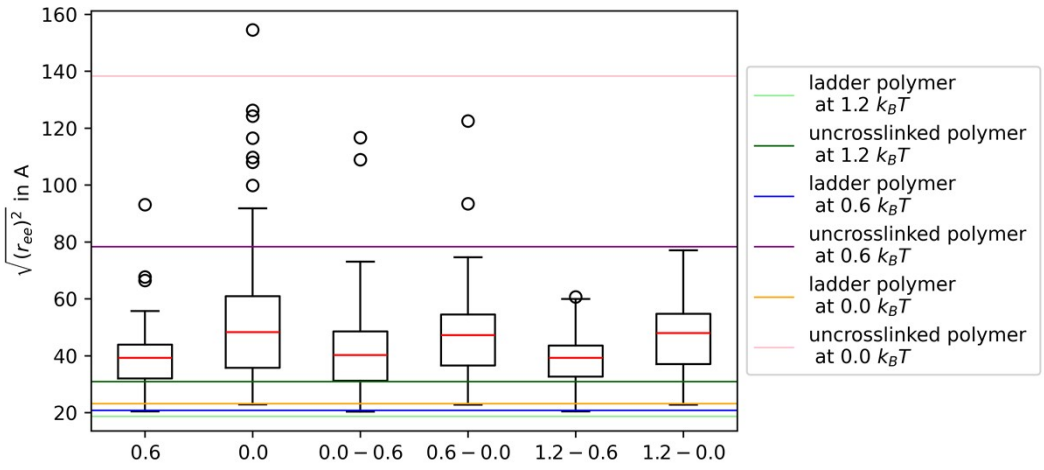

(a) end-to-end-distances.

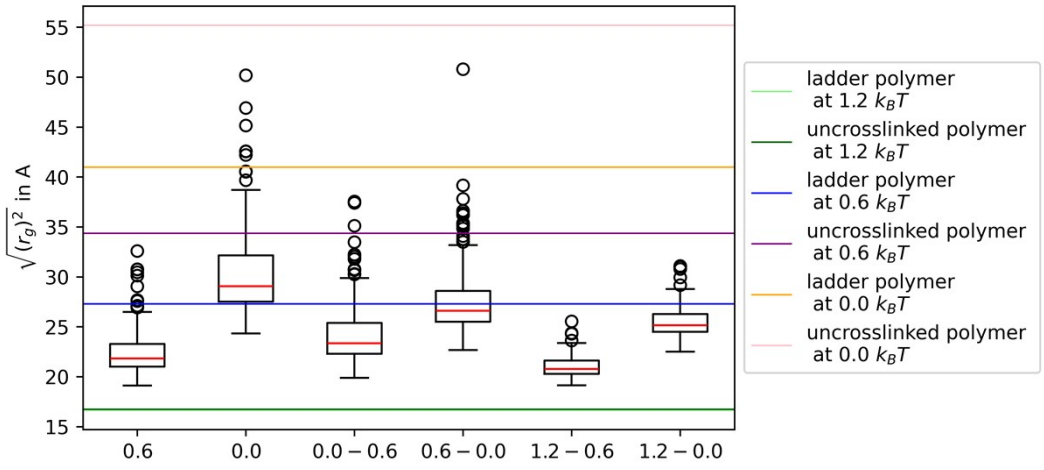

(b) radii of gyration.

Fig. S7: Comparison of the radii of gyration and end-to-end distances of the randomly linked polymers with the values of the ladder polymers (the indicated ϵ (in ^{k_BT}) in was kept both for dynamic SCNP synthesis and analysis after SCNP formation on the left hand side, while the synthesis conditions were reversed for the right hand side, i.e. "$0.0 - 0.6$" indicates a synthesis at $\epsilon = 0.0\ k_BT$, but an equilibration and analysis at $^{0.6\ k_BT}$); marked in orange is the median and the middle 50 % of all values are located within the box; the bar is limited by the upper and lower statistical outlier limits, whose distance from the box corresponds to a maximum of one and a half times the length of the box; the points outside the outlier limits are "rogue results" that deviate significantly from the other values; the yellow and blue markings correspond to the mean value for the "presynthesized" ladder polymer (the values for the parental diblock are also indicated).

Kinetics

The contents of Fig. 7 (c) (main part) is shown in a non-logarithmic representation in Fig. S8.

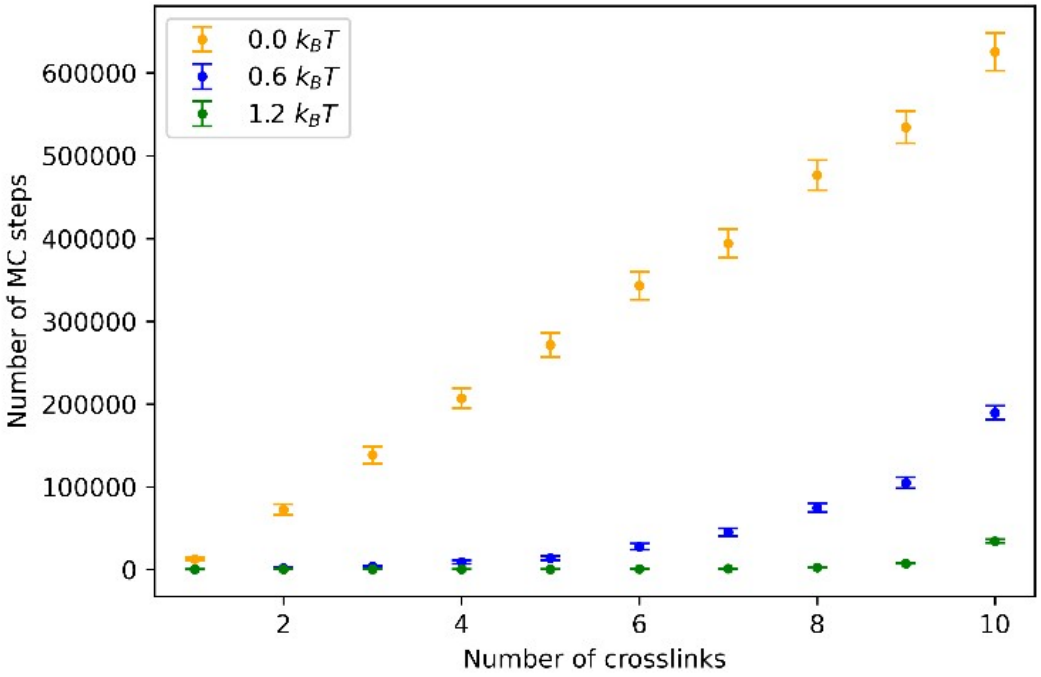

Fig. S8: number of average MC steps in which the *n*-th crosslink was set (non-logarithmic representation of Fig. 7 c) in main part).

Finally, the full kinetics of crosslinking is represented in Fig. S9 for setting the *n*-th crosslink.

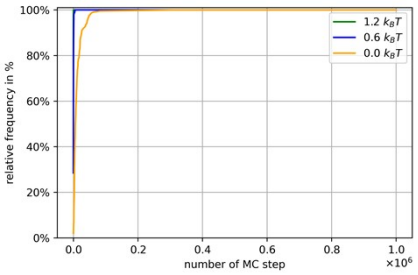

(a) MC step of first crosslink.

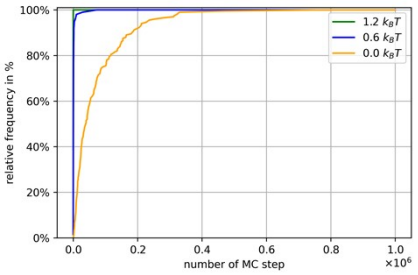

(b) MC step of second crosslink.

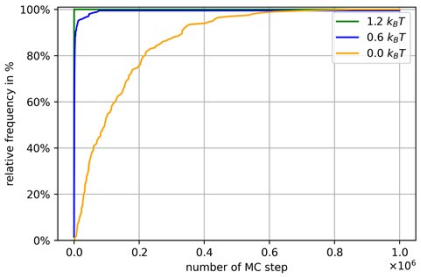

(c) MC step of third crosslink.

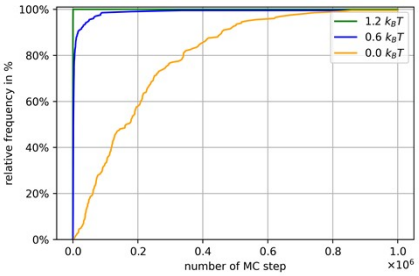

(d) MC step of fourth crosslink.

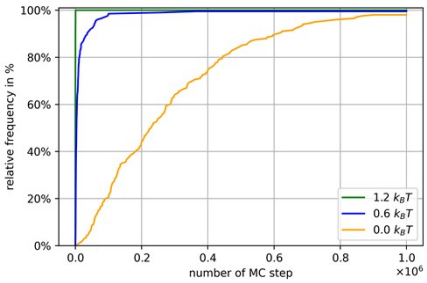

(e) MC step of fifth crosslink.

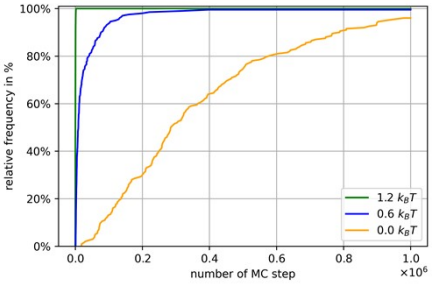

(f) MC step of sixth crosslink.

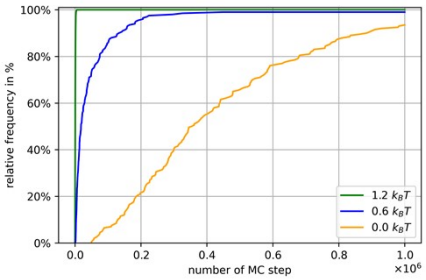

(g) MC step of seventh crosslink.

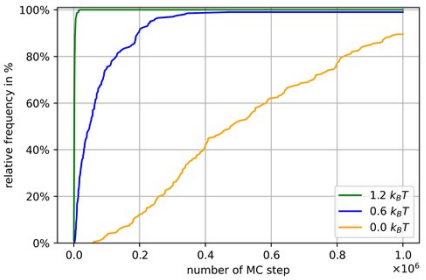

(h) MC step of eighth crosslink.

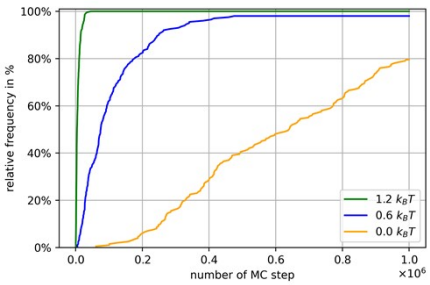

(i) MC step of ninth crosslink.

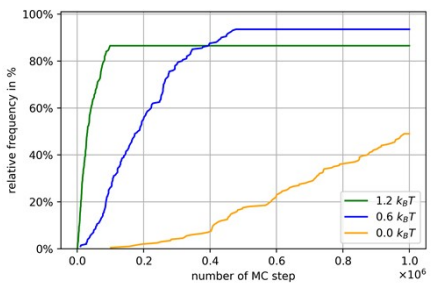

(j) MC step of tenth crosslink.

Fig. S9: Percentage of simulations having set the *n*-th crosslink at a certain MC step for three different interaction strengths.

Scattering

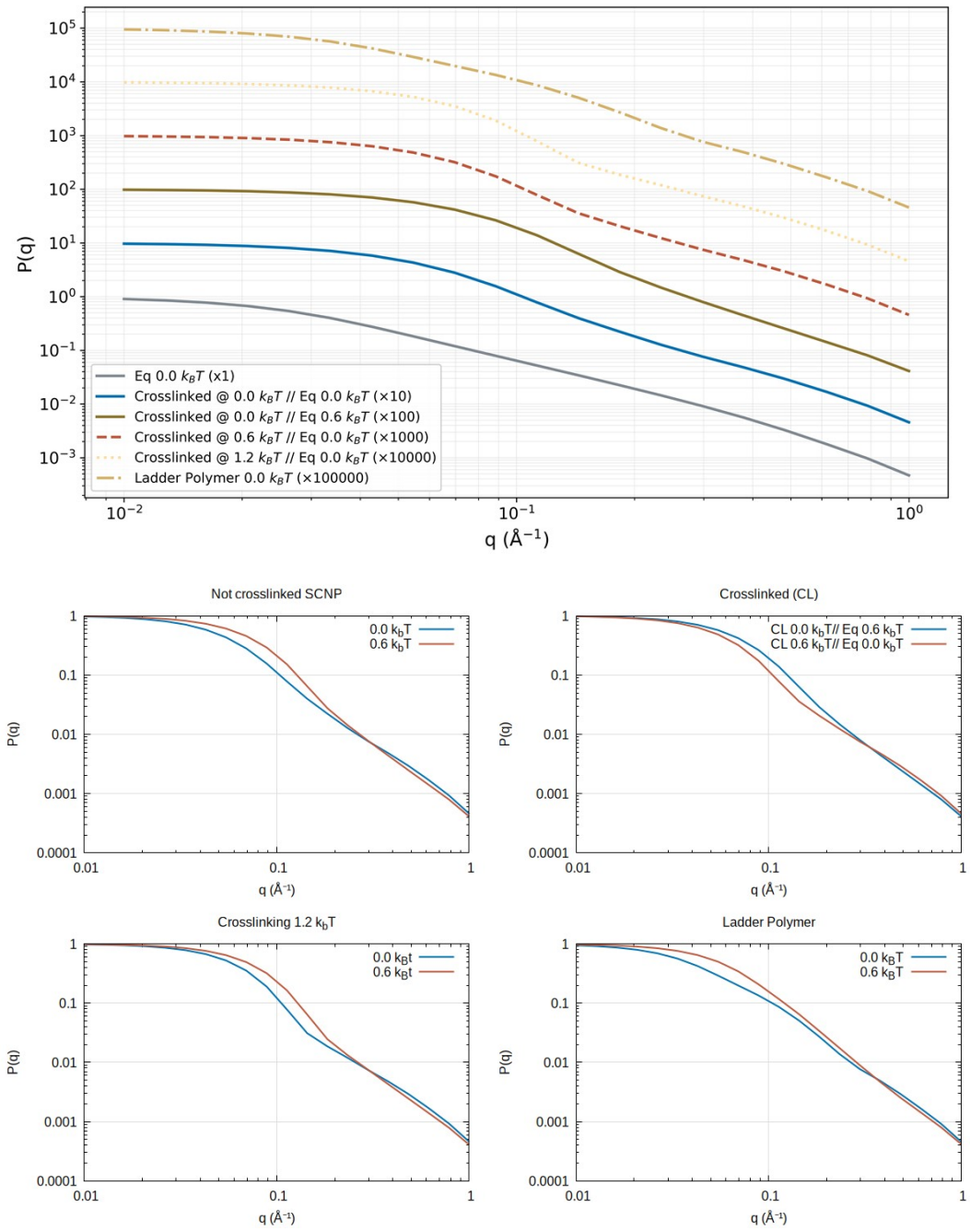

Fig. S10: Different representations of the form factors depicted also partly in the main part.

Comparison with Molecular Dynamics simulations

For comparison with the results from Monte Carlo simulations described in the main text, we also performed molecular dynamics simulations for a very similar model. The main difference is that, for technical reasons, we used differentiable potentials in the MD simulations.

For the diblock copolymer we used a bead-spring model for polymers consisting of 100 consecutive beads of type A and 100 consecutive beads of type B. All beads interact with a Weeks-Chandler-Anderson excluded volume potential,

$$u_{WCA}(r_{ij}) = f(x) = \begin{cases} 4\epsilon_{WCA} \cdot \left(\left(\frac{\sigma}{r_{ij}}\right)^{12} - \left(\frac{\sigma}{r_{ij}}\right)^{6}\right) + \epsilon_{WCA}, & r_{ij} \leq 2^{\frac{1}{6}}\sigma \\ 0, & r_{ij} > 2^{\frac{1}{6}}\sigma \end{cases}$$

where σ is the bead diameter, $\epsilon_{WCA} = 1k_BT$ quantifies the depth of the potential and r_{ij} is the distance between beads i and j. Consecutive beads along the polymer chain additionally interact with a harmonic bond potential according to

$$u_{bond} = \frac{k}{2}(r_{ij} - r_0)^2$$

We chose a spring constant of $k = 16k_BT/\sigma^2$ and an equilibrium distance of $r_0 = 1.25\,\sigma$.

To mimic an attractive interaction of beads of type A with beads of type B, we used an additional truncated and shifted Lennard-Jones potential, with potential depths of 0.0 k_BT, 0.6 k_BT and 1.2 k_BT. The $\epsilon_{3\sigma} \approx 0.00548\,\epsilon$ parameter ensures the potential remains continuous.

$$u_{LJ}(r_{ij}) = f(x) = \begin{cases} 4\epsilon \cdot \left(\left(\frac{\sigma}{r_{ij}}\right)^{12} - \left(\frac{\sigma}{r_{ij}}\right)^{6}\right) + \epsilon_{3\sigma}, & r_{ij} \leq 3\sigma \\ 0, & r_{ij} > 3\sigma \end{cases}$$

Equal to the model described in the main text every fifth bead was chosen to be a crosslinkable bead. All interaction potentials of the crosslinker beads were otherwise equal to those of the other beads in the same block.

We used reduced units with $\tau = 1$, $T = 1$, $m = 1$, $\sigma = 1$ and enforced an NVT ensemble using a Nosé-Hoover thermostat.[2] The time integration is performed with a timestep of $t = 0.005\tau$. Equal to the procedure described for the MC simulations, a permanent crosslink was set, when crosslinkable beads of different types approached to a distance smaller or equal the minimal crosslinking distance $r_{\text{distcl}} = 1.5\,\sigma$ or $r_{\text{distcl}} = 1.25\,\sigma$ in the case of $\varepsilon = 1.2k_BT$. Each simulation consisted of 106 timesteps for equilibration, 10^6 timesteps for crosslinking, $5 \cdot 10^5$ timesteps for equilibrating the crosslinked SCN without the attractive potential and finally , $5 \cdot 10^5$ timesteps for the evaluation of R_G and R_{ee}.

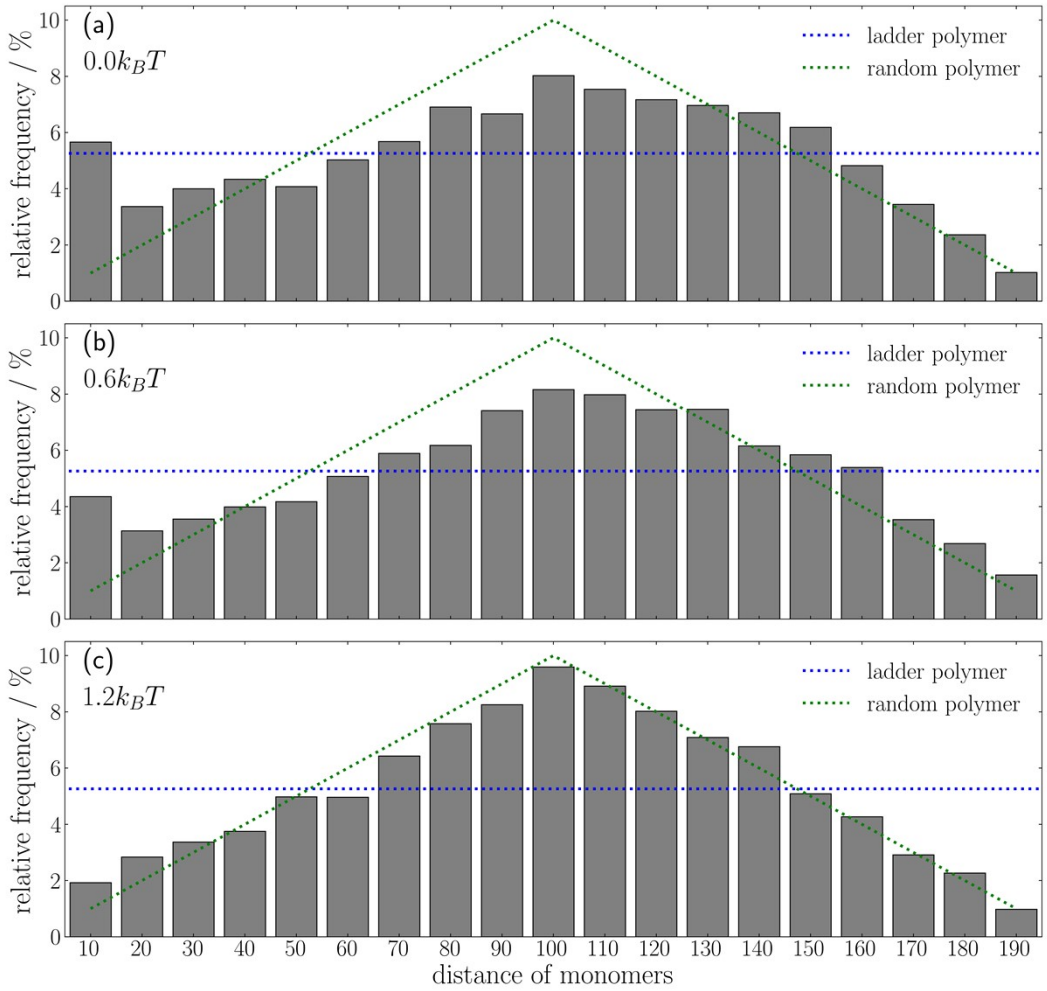

Fig. S11: Histogram of probabilities of finding certain distances along the chain (in number of monomers) between two mutually crosslinked monomers as seen by reactive MD simulations (top: synthesis at low attractive interaction potential; center: at medium interaction potential; bottom: at high attractive interaction potential between the blocks; lines are give as reference as for the figure in the main part).

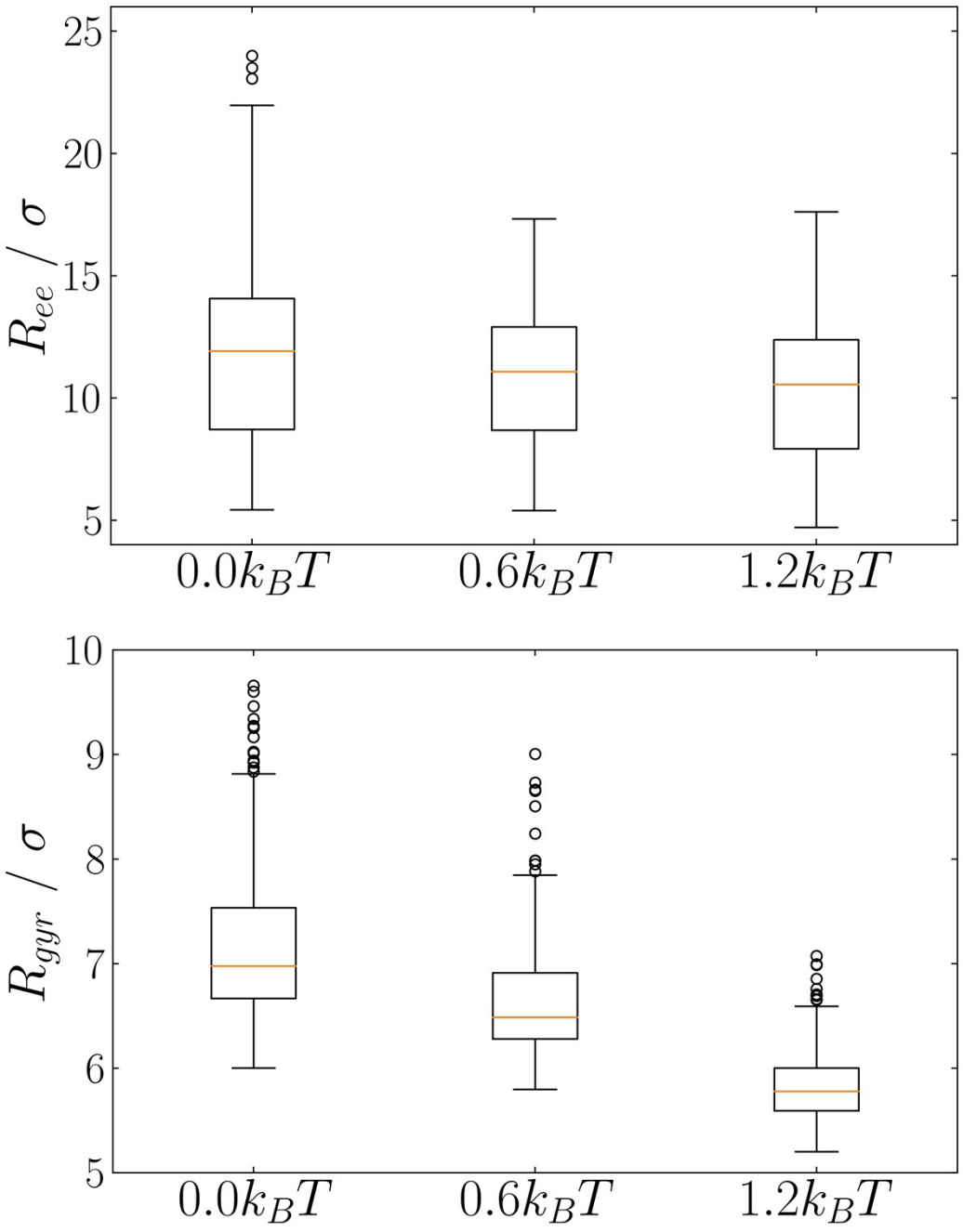

Fig. S12: Representation of end-to-end distances and radii of gyration obtained from reactive MD simulations in dependence of the interaction potential during "synthesis" and measured after equilibration at vanishing interaction potential.

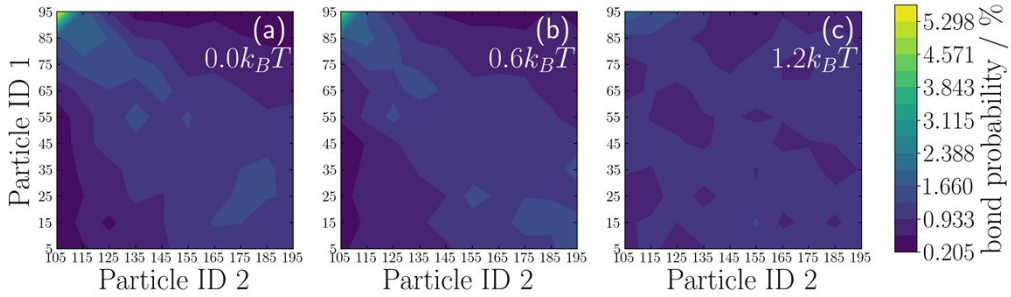

Fig. S13: Heatmaps, whose "brightness" is proportional to the frequency of finally established crosslinks of a basically fully crosslinked SCNP (center) obtained from reactive MD simulations; all simulation "reactions" at $\epsilon = 0.0\ k_BT$ (left), at $\epsilon = 0.6\ k_BT$ (center) or at $\epsilon = 1.2\ k_BT$ (right).

References

(1) Hebbeker, P.; Plamper, F. A.; Schneider, S. Effect of the Molecular Architecture on the Internal Complexation Behavior of Linear Copolymers and Miktoarm Star Polymers. *Macromol. Theory Simul.* **2015**, *24* (2), 110–116. DOI: 10.1002/mats.201400077.

(2) Shinoda, W.; Shiga, M.; Mikami, M. Rapid estimation of elastic constants by molecular dynamics simulation under constant stress. *Phys. Rev. B* **2004**, *69* (13), 134103. DOI: 10.1103/PhysRevB.69.134103.